Design and implementation of a novel inertia flywheel pendulum mechatronic kit

Article *in* Journal of Vibration and Control · January 2014

DOI: 10.1177/1077546314524973

3 authors, including:

Jonqlan Lin
Chien Hsin University of Science and Technology
53 PUBLICATIONS **544** CITATIONS

SEE PROFILE

Wei-Hsin Gau
Huafan University
27 PUBLICATIONS **101** CITATIONS

SEE PROFILE

Article

Journal of Vibration and Control
2015, Vol. 21(16) 3417–3430

DOI: 10.1177/1077546314524973
jvc.sagepub.com

Design and implementation of a novel inertia flywheel pendulum mechatronic kit

Jonqlan Lin[1], Shin Yuan Chen[1] and Wei-Hsin Gau[2]

Abstract

The inertia flywheel pendulum exhibits several characteristics, such as underactuation and nonlinearity, that make it attractive for research and advanced control education. The main goal of this paper is to develop a novel mechatronic kit with a control methodology for an inertia flywheel pendulum. The mechatronic kit has a motor and flywheel mounted at the top of the body. It is a physical pendulum with a symmetric wheel attached to the end, which is free to spin around an axis parallel to the axis of rotation of the pendulum. The flywheel is actuated by a direct current motor and the coupling torque generated by angular acceleration of a wheel disk is used to dynamically control the system. The hybrid control strategy for stabilization of the inertia flywheel pendulum is presented and examined. The control aim is achieved by the solution of the following two particular control problems: swinging the pendulum up to a certain neighborhood of the inverted position and balancing it in this position. The energy control was designed for swing-up of the inverted pendulum. The genetic algorithm proportional-integral-derivative controller was implemented for balancing the inverted pendulum. The proposed hybrid control methodology has successfully performed stabilization control, even when unexpected loading conditions occur. Consequently, the novel flywheel pendulum system is ideally suited for advanced control courses for educating university students.

Keywords

Energy control, flywheel, genetic algorithm, hybrid control, inverted pendulum

1. Introduction

The control of oscillatory mechatronic systems has received increasing attention from a theoretical perspective. Numerous laboratory control kits have been developed for research and educational purposes. As a typical problem in dynamics and control theory, the inverted pendulum is generally used as a benchmark for evaluating control algorithms. This pendulum has highly coupled, multi-variable, intrinsically nonlinear, and unstable features. Conventionally adopted inverted pendulums predominantly maintain their stability by moving horizontally at the base. However, with the exploration of robotic unicycles (Lam, 2011) or biped robots, their balance control is impossible simply through the model of conventionally adopted inverted pendulums. For instance, Lam (2011) used a reaction wheel mounted in the robot's body as a torque generator to balance itself. Hence, this inertia flywheel pendulum offers a different viewpoint towards solving problems related to this robotic system.

From a pedagogical standpoint, the inertia flywheel pendulum is a simple nonlinear system, illustrating advanced control designs based on geometric methods (Spong et al., 2001). In contrast to the traditional inverted pendulum, the inertia flywheel pendulum is characterized by its simple design, nonlinear properties, and complex control methodology. An inertia flywheel pendulum system generally has fewer independent

[1]Department of Mechanical Engineering, Chien Hsin University of Science and Technology, Taiwan
[2]Department of Mechatronic Engineering, Huafan University, Taiwan

Received: 21 October 2013; accepted: 27 January 2014

Corresponding author:
Jonqlan Lin, Department of Mechanical Engineering, Chien Hsin University of Science and Technology, 229 Chien-Hsin Road, Jung-Li City, 320, Taiwan.
Email: jlin@uch.edu.tw

control actuators than degrees of freedom, which is known as an underactuated system (Aoustin et al., 2006). The inertia flywheel pendulum is located at the stationary end, which is motor driven. Thus, the flywheel is actuated while the pendulum is idle. The coupling torque generated by angular acceleration of a wheel disk is used to actively control the system.

Stabilizing an underactuated system is extremely difficult. Developing stabilizing algorithms for flywheel-type pendulum systems that use nonlinear control laws has received considerable interest (Spong et al., 2001) – neural networks (Chetouane and Darenfed, 2008), fuzzy controllers (Chetouane et al., 2010; Ruan and Wang, 2010), neural-adaptive output feedback controls (Li and Yang, 2012), energy-based controls (Fantoni et al., 2001; Grishin et al., 2002), and variable structure controls (Aguilar et al., 2009).

A previous work demonstrated the feasibility of stabilizing the unstable equilibriums of a two-link pendulum with a flywheel (Aoustin et al., 2005). Additionally, in addition to the establishment of the planar dynamic model by the Lagrange equation, a previous work developed a fuzzy controller based on packet control to achieve balanced control of a flywheel inverted pendulum system (Ruan and Wang, 2010). However, the above works lack experimental verification and demonstrate simulation results only. Srinivas and Behera (2008) devised two swing-up control strategies for a reaction wheel pendulum. Aguilar et al. (2009) developed an effective means of generating a self-excited oscillation for an inertia wheel pendulum through means of a variable structure controller. All control approaches are implemented on a mechatronics control kKit provided by Quanser Inc.

An inverted gyroscopic pendulum (GIP), which is freestanding, is another reaction wheel pendulum. The fulcrum is a V-shaped groove at the base, which allows one degree of freedom (Chetouane and Darenfed, 2008; Chetouane et al., 2010). However, the proposed GIP scheme is limited in that the fulcrum is kept in a groove, allowing it to move freely only on either side. Previous works developed a reaction wheel pendulum on a movable platform (Li and Yang, 2012; Formal'sky, 2006; Pyrkin et al., 2009). Hence, developing an inertia flywheel pendulum mechatronic kit is still a promising topic for advanced control courses. Moreover, according to the above literature review, a hybrid control strategy for stabilizing such a system is under development.

Therefore, this work presents a novel mechatronic kit with a control methodology for an inertia flywheel pendulum. The rest of this paper is organized as follows. Section 2 introduces the inertia flywheel pendulum model. Section 3 then describes the system configuration for such an inertia flywheel pendulum. Section 4 presents the hybrid control structure, which consists of swing-up, standing-up and balancing features to stabilize the pendulum at the top equilibrium point. Section 5 summarizes our experimental results and offers concluding remarks.

2. Dynamics modeling

Figure 1 schematically depicts an inertia flywheel pendulum. The Lagrangian formulation is a feasible means of deriving the equations of motion for mechatronic systems such as the inertia flywheel pendulum. The dynamic equation for the inertia wheel pendulum can be modeled as a two-link robot, in which the pendulum forms the first link and the flywheel outlines the second one. The center of mass of the flywheel is generally assumed to be coincident with the axis of rotation and measure the angle of the pendulum clockwise from the vertical direction. With two degrees of freedom, the inertia flywheel pendulum takes generalized coordinates as the angles θ_p f the pendulum and θ_f f the flywheel (Figure 1).

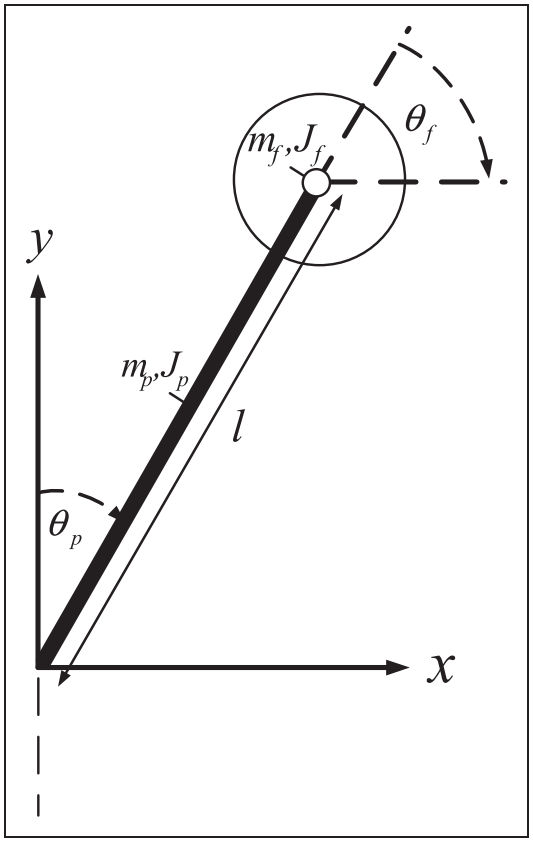

Figure 1. Schematic diagram of the inertia flywheel pendulum.

Kinetic energy, K, of the proposed system is the sum of the pendulum kinetic energy and the flywheel kinetic energy, and is written as

$$K = \frac{1}{8}m_p l^2\dot{\theta}_p^2 + \frac{1}{2}m_f l^2\dot{\theta}_p^2 + \frac{1}{2}J_p\dot{\theta}_p^2 + \frac{1}{2}J_f(\dot{\theta}_p + \dot{\theta}_f)^2 = \frac{1}{2}J\dot{\theta}_p^2 + \frac{1}{2}J_f\dot{\theta}_t^2 \quad (1)$$

where

$$\theta_t = \theta_p + \theta_f,$$
$$J = J_p + m_p\left(\frac{1}{2}l\right)^2 + m_f l^2.$$

Additionally, the potential energy, P, of the system is assumed here to be due only to gravity. Although elasticity of the motor shaft or pendulum link results in additional potential energy terms, these effects are assumed here to be negligible. Thus, the potential energy is

$$P = mgl(1 - \cos\theta_p) \quad (2)$$

where $m = m_p + m_f$

Once the kinetic and potential energies are determined, the equations of motion are expressed based on Lagrange's formulation. In such cases, the torque produced by the motor in a torque u is applied on a flywheel, and $-u$ acts on the pendulum. Hence, the equations of motion are described as

$$\begin{aligned} J\ddot{\theta}_p + mgl\sin\theta_p &= -u \\ J_f\ddot{\theta}_t &= u. \end{aligned} \quad (3)$$

Notably, the frequency of oscillation for the pendulum in small amplitudes is $\omega_p = \sqrt{mgl/J}$. Moreover, the second equation of equation (3) is simply a double integrator. For small values, θ_p function $\sin\theta_p$ are approximated by argument θ_p. Consequently, the approximated linearized system of equation (3) around the top equilibrium point can be expressed as

$$\begin{aligned} J\ddot{\theta}_p + mgl\theta_p &= -u \\ J_f\ddot{\theta}_t &= u \end{aligned} \quad (4)$$

By introducing the state variables $x = \begin{bmatrix}\theta_p & \theta_t & \dot{\theta}_p & \dot{\theta}_t\end{bmatrix}^{\mathrm{T}}$ and the system output $y = \theta_p$, equation (4) should be rewritten as

$$\dot{x} = \begin{bmatrix} 0 & 0 & 1 & 0 \\ 0 & 0 & 0 & 1 \\ -mgl/J & 0 & 0 & 0 \\ 0 & 0 & 0 & 0 \end{bmatrix}\begin{bmatrix}\theta_p \\ \theta_t \\ \dot{\theta}_p \\ \dot{\theta}_t\end{bmatrix} + \begin{bmatrix} 0 \\ 0 \\ -1/J \\ -1/J_f \end{bmatrix}u = Ax + Bu$$
$$y = \theta_p = Cx \quad (5)$$

The controllability matrix in $\mathbf{C_M} = \begin{pmatrix} B & AB & A^2B & A^3B \end{pmatrix}$ is full rank and, thus, the system is controllable. This finding implies that the dynamics of the closed-loop system can be shaped arbitrarily by using only one control variable.

3. System configuration

Figure 2 schematically depicts the inertia flywheel pendulum, while Figure 3 displays the exploded view of the mechatronic system. The system has a motor and flywheel mounted at the top of the body. Additionally, the system is a physical pendulum with a symmetric wheel attached to the end, which is free to spin around an axis parallel to the axis of rotation of the pendulum. The wheel is actuated by a direct current (DC) motor, and the coupling torque is generated by the angular acceleration of a wheel that can be used to dynamically control the system. Assume that such a mechanism is present in zero gravity. If the flywheel is forced to rotate in the clockwise direction, the pendulum link rotates in the opposite direction, thus conserving the angular momentum around the center of gravity of the whole assembly (Figure 4).

The entire system is installed in the Sensor and Control Laboratory in the Department of Mechanical Engineering of Chien Hsin University of Science and Technology. Figure 5 illustrates the experimental apparatus. The pendulum and its support tower are made of aluminum alloy, making it a lightweight device. Moreover, this kit has a high-resolution optical encoder fitted onto the axis. A digital/analog (D/A) converter provides a current command voltage to an amplifier that drives the brushless DC motor (BLDC). Additionally, by using a rotary connector, this apparatus links the motor power supply and encoder signals to ensure unlimited rotation of the pendulum motion. Moreover, the controller is implemented in the MATLAB/SIMULINK real-time workshop with a sample interval of 1 ms. Angular rates are estimated using a first-order difference with no filtering. The restoring torque depends on the movement of the flywheel. The brushless DC motor must be run in a Min-Max voltage limit. Therefore, the proposed inertia flywheel inverted pendulum is a novel and challenging platform to design and evaluate several control synthesis approaches.

4. Controller design

The inertia flywheel pendulum system sustains a balance from the adaptation of the rotation velocity of the flywheel rather than by moving the base that is typical to balance control for the conventional inverted pendulum. The control goal of such a system is to swing

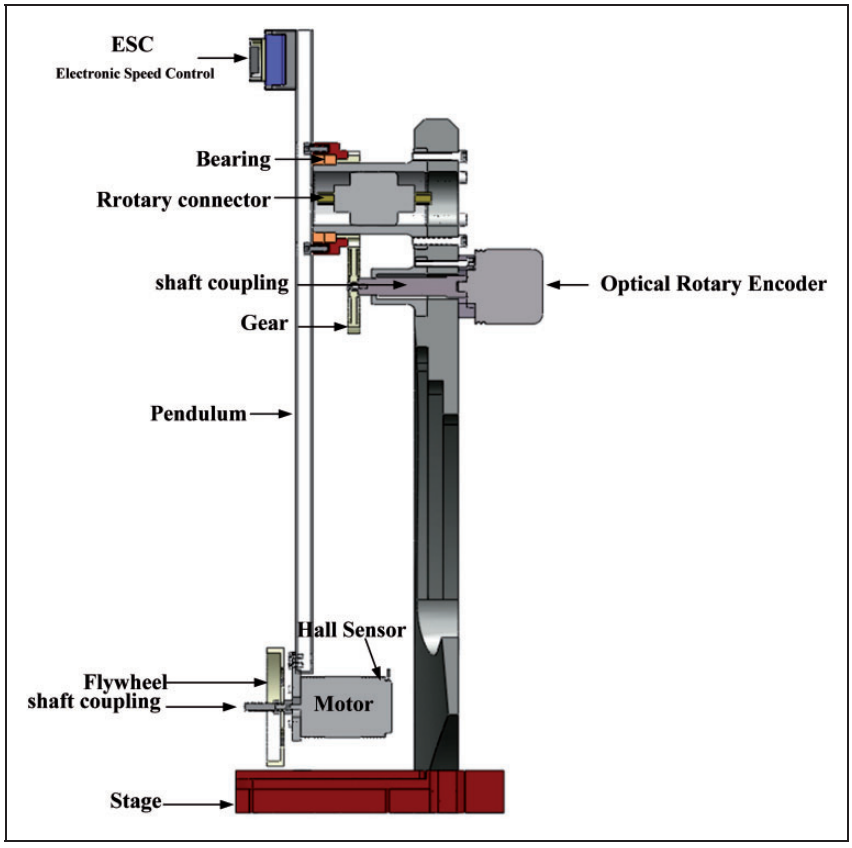

Figure 2. The configuration of the proposed inertia flywheel pendulum.

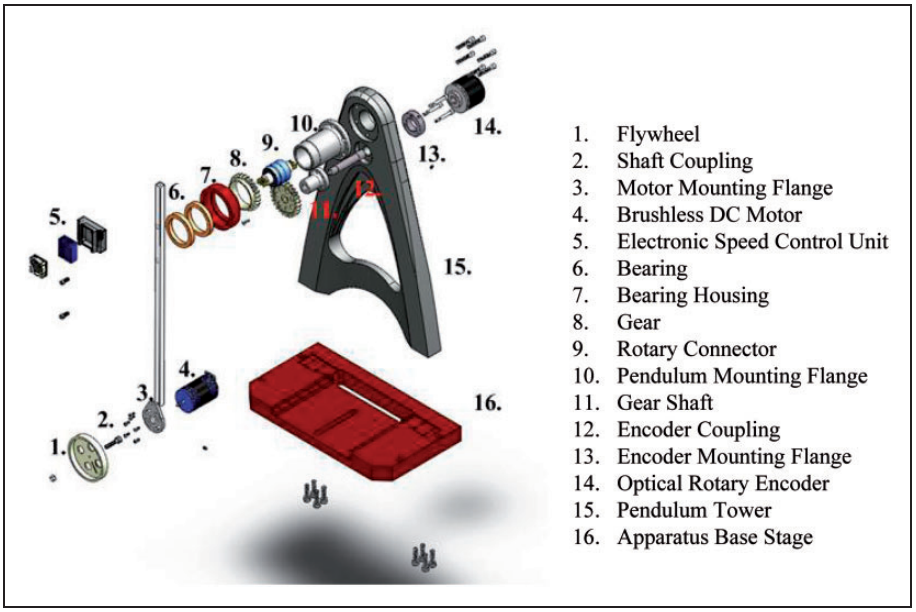

Figure 3. Exploded views of the proposed inertia flywheel pendulum.

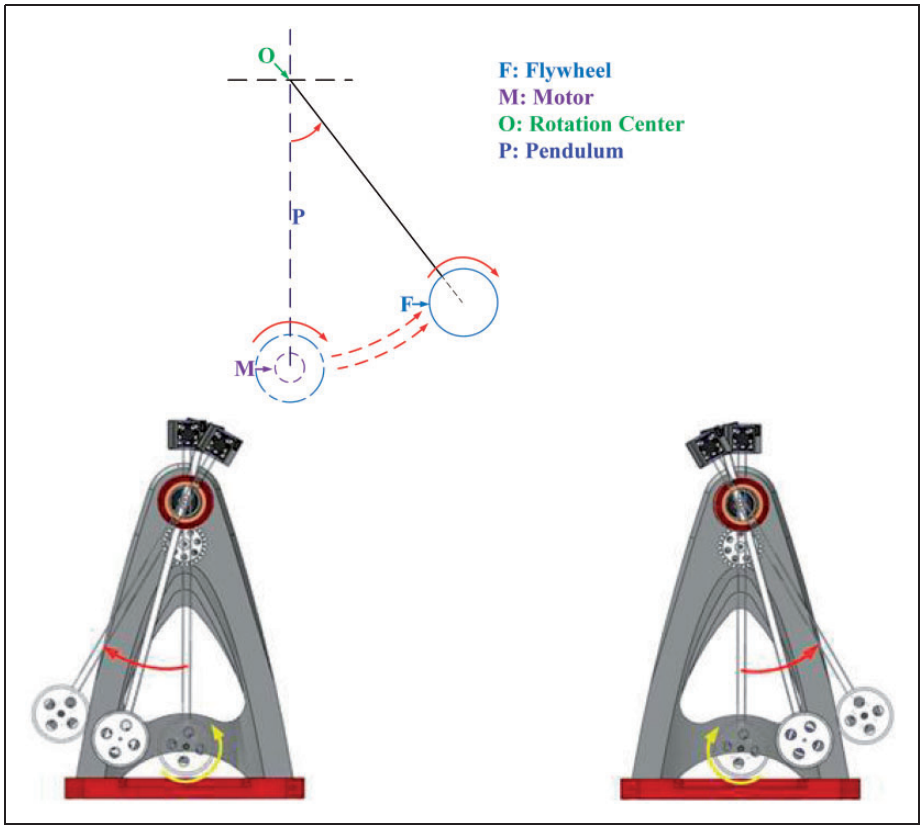

Figure 4. Motion concept for inertia flywheel pendulum.

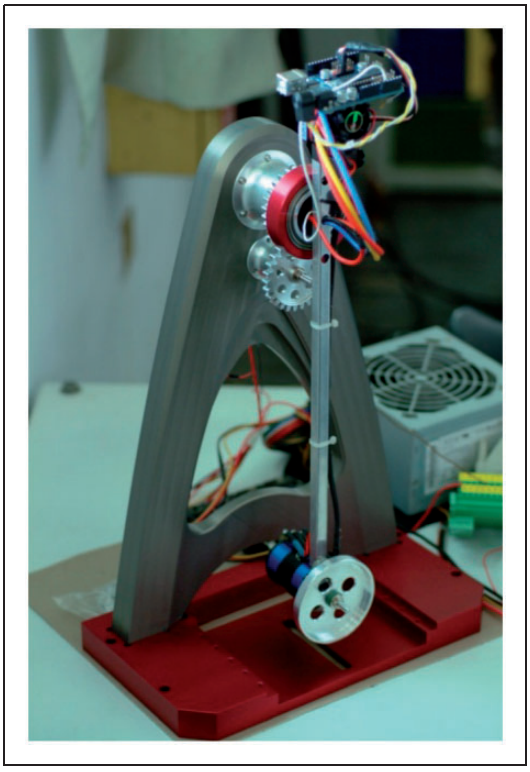

Figure 5. Experimental apparatus for inertia flywheel pendulum.

the pendulum from the downward stable equilibrium position to the top unstable equilibrium point. Hence, based on the control structure, this work develops hybrid control modes that consist of swing-up, standing-up and balancing to stabilize the pendulum at the top equilibrium point. The proposed algorithm must solve the following subtasks: placing the pendulum in the neighborhood of the desired equilibrium point, standing-up, and balancing around this position (Figure 6). As swing-up control takes the pendulum near the upright position, the standing-up, and balancing (stabilization) control is activated. The control scheme involves switching from energy control to the stabilization control mode in order to set it upright the pendulum (Figure 6). Therefore, the control scheme switches to the stabilization control mode in order to balance the pendulum at the top position.

4.1. Swing-up control

The swing-up control problem moves the pendulum from the downward position by hanging the position up into the inverted position. The swing-up control strategy treats oscillations as perturbations from the downward stable equilibrium point. The pendulum swings in a clockwise or an anti-clockwise direction until it nearly reaches the top equilibrium position.

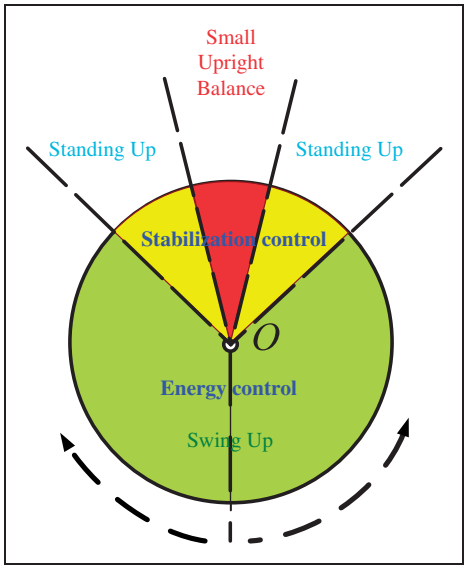

Figure 6. Hybrid control modes.

However, this control scheme takes the pendulum from the downward bottom position to the upward top position in a single swing, which demands an extremely high torque. Therefore, this work introduces an energy control strategy and demonstrates the feasibility of using this swing-up idea to control the large angular movements of a pendulum.

The objective function appears as

$$H(\theta_p, \dot{\theta}_p) = \frac{1}{2}\Delta E^2(t), \tag{6}$$

where $\Delta E(t) = E - E_r$.

Thus, the scaled energy E is defined as

$$E = mgl(1 - \cos\theta_p) + \frac{1}{2}J\dot{\theta}_p^2. \tag{7}$$

Moreover, reference energy E_r is 2 mgl when the pendulum is hanging down and 0 when the pendulum is upright. This energy control strategy brings the energy of the pendulum to reference value E_r and, simultaneously, brings the wheel speed to zero.

Equation (6) indicates that the reference energy level can be decreased until this level is insufficient to bring the pendulum to top equilibrium neighborhood. Consequently, the control law obtained from the formula of speed gradient approach has the following form (Pyrkin et al., 2009):

$$u_1 = \gamma\Delta E(t)\sigma, \tag{8}$$

where γ denotes an arbitrary positive constants, and $\sigma = \frac{\partial \dot{E}}{\partial u_1}$.

Therefore, the energy control strategy has the form

$$u_1 = \gamma\left(\frac{1}{2}J\dot{\theta}_p^2 - mgl(1 + \cos\theta_p)\right)\dot{\theta}_p \tag{9}$$

However, the swing-up controller fails to balance the pendulum, owing to the fact that it can only swing the pendulum up to a neighborhood of the equilibrium starting from arbitrary initial conditions. A stabilization controller is thus necessary for this system.

4.2. Stabilization control

As the above controller design suggests, the energy control strategy strives to swing the pendulum from hanging down to going up. However, the energy controller moves the pendulum near the inverted configuration for initial conditions yet cannot balance it there. An effective strategy utilizes the energy control until the pendulum is close to the inverted position and the switch control to the local stabilizing control. Therefore, switching control is introduced into the system. Ultimately, a control strategy must be identified that keeps the pendulum upright.

Firstly, it is desirable to avoid transients while switching between controllers. Therefore, a stabilization controller is chosen to allow the vector field of the system with the stabilization controller to match the homo-clinic orbit when the pendulum is upright. The energy controller drives the pendulum to a homo-clinic orbit given by $E = 2mgl$, implying that (Block et al., 2007)

$$mgl(1 - \cos\theta) + \frac{1}{2}J\dot{\theta}^2 = 2mgl \tag{10}$$

Solving for $\dot{\theta}$ from equation (10) and gives

$$\dot{\theta} = \sqrt{\frac{2mgl}{J}(1 + \cos\theta)} = \omega_p\sqrt{2(1 + \cos\theta)} \tag{11}$$

Moreover, the pendulum approaches the upright position along the straight line

$$\frac{\dot{\theta}}{\omega_p} = 2\pi - \theta. \tag{12}$$

Additionally, this work provides conditions for switching from stabilization to energy control. Assuming that the linear model is sufficiently accurate and that the flywheel velocity is sufficiently small allows us to infer that a linear strategy, which is correlated with the homo-clinic orbit, stabilizes the system if

$$\left|\dot{\theta}_p - \omega_p\theta_p\right| < \frac{J_p}{\omega_p}u_{\max} \tag{13}$$

Where $u_{\max}$ denotes the largest control signal (Block et al., 2007). Thus, equation (13) is the switching condition from stabilization to energy control. While the state moves outside the region (13), the pendulum falls down quickly.

Therefore, this subsection introduces a control algorithm to obtain a near optimum proportional-integral-derivative (PID) controller for the stabilization controller design. The second-order transfer function from (5) is

$$\mathbf{G}_{CL}(s) = C(s\mathbf{I} - A)^{-1}B \tag{14}$$

In the pendulum stabilization control task at the top equilibrium, the main control purpose is expressed by the limitation equation:

$$\lim_{t\to\infty} e = \lim_{t\to\infty}(\theta_p(t) - \theta^*) = 0, \tag{15}$$

where $\theta_p(t)$ denotes the current pendulum angle, and θ^* represents the desired pendulum angle corresponding to an unstable equilibrium. Generally, the desired pendulum angle θ^* is always set to zero.

Moreover, the PID standard form is

$$u_2 = -K_p e - \frac{K_i}{s}e - K_d s e \tag{16}$$

where e denotes the tracking error signal; u_2 represents the stabilization control action; and K_p, K_i, and K_d, refer to the proportional, integral, and derivative gain, respectively.

Therefore, the parameters of PID control, based on genetic algorithm (GA) are introduced to find the near-optimum feedback controller. The following derivation procedure resembles that of Lin and Zheng (2012). Details of the fundamental working principles for the proposed GA PID control can also be found in Lin and Zheng (2012). The GA uses the coding of the parameter set to determine the concentrations of the near optimum points. A previous work suggested that the optimization problem for selecting the control parameters can be expressed as (Lin and Zheng, 2012)

$$\min \left\| \mathbf{G}_{CL}(j\omega_n) \right\|. \tag{17}$$

where the H_∞-norm of the closed-loop transfer function is to be minimized.

Additionally, the objective function depends on the specific problem to be optimized, and defined as

$$OBJ = \sqrt{\frac{\sum_{i=1}^{N}(y_i - \hat{y}_i)^2}{\sum_{i=1}^{N} y_i^2}} \tag{18}$$

where y_i denotes the measured response, and $\hat{y}_i$ refers to the estimated response. The algorithm starts with random initial values and attains the objective function value for each gene.

Moreover, performance of the proposed control scheme is evaluated, in which the GA model used here is given a crossover rate of 0.9 and a mutation rate of 0.03 to first seek the near-optimum PID controller. The population size is set at 50, and the maximum number of generations is set at 30.

4.3. Hybrid control

The complete hybrid control for the calculated control signal is presented below:

$$u(t) = \begin{cases} u_1(t), \left|\theta_p - 2\pi\right| \geq \theta_s, \\ u_2(t), \left|\theta_p - 2\pi\right| \leq \theta_s, \end{cases} \tag{19}$$

where $u_1(t)$ and $u_2(t)$ represent the energy control algorithm (i.e. swing-up) (equation 9) and the stabilization control algorithm (i.e. standing-up and balancing) (equation 16); and θ_s denotes the pendulum angle when switching has occurred between two algorithms.

5. Results and discussions

5.1. Implementation of the mechatronic control kit

The control algorithms are implemented with the Arduino control board using the MATLAB/SIMULINK real-time workshop. Figure 7 illustrates the developed inertia flywheel pendulum mechatronic kit. The control voltage is generated by the Arduino control card and sent pulse-width-modulation (PWM) control signals to ESC. The Arduino control card in this implementation is characterized by its low price, small size, and flexibility for control purposes. As an electronic circuit that varies the speed of a motor, ESC is often used for the BLDC motor (model: GENESE 60A 10.5R; specifications: KV = 3500, power = 190 W, weight = 189 g), which provide an electronically generated three-phase electric power low voltage source of energy for the motor. Also, the rotation angle of the pendulum is sensed using the rotary incremental encoder (model: HONTKO HTR-W-500-3).

Moreover, size dimension is a priority concern in flywheel design. Acquiring lightweight flywheels involves drilling holes in the flywheel. The flywheel parameters are a weight of 39 g, an outside diameter of 75 mm, thickness of 3 mm, and center-hole diameter of 3 mm. Additionally, measuring the dimensions of the components, weighing them, and computing

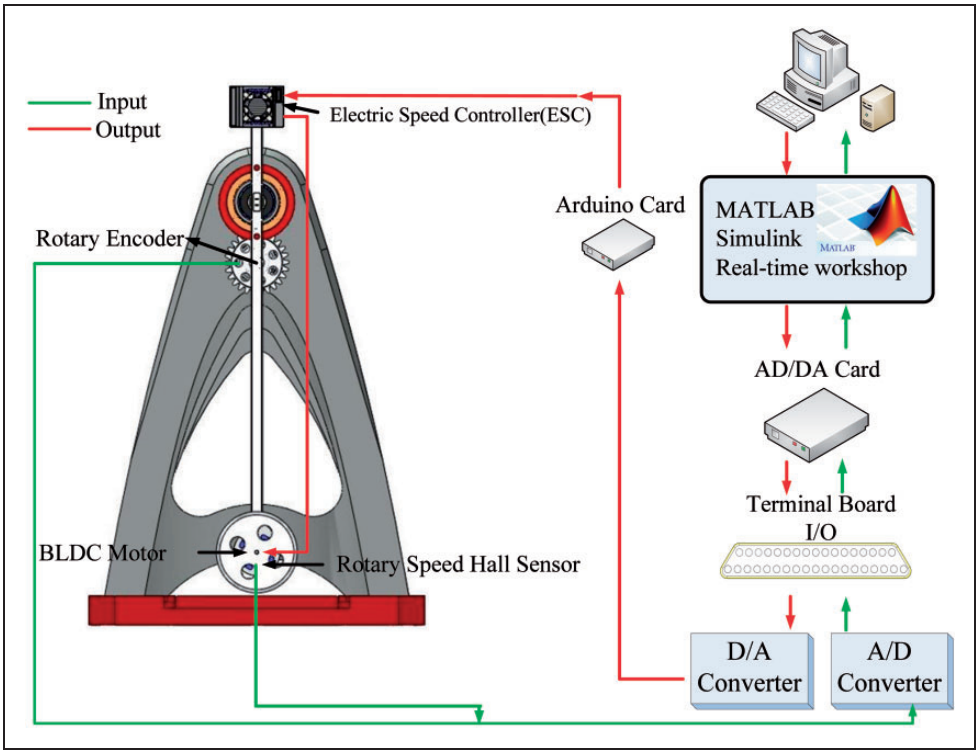

Figure 7. Implementation of the inertia flywheel pendulum mechatronic kit.

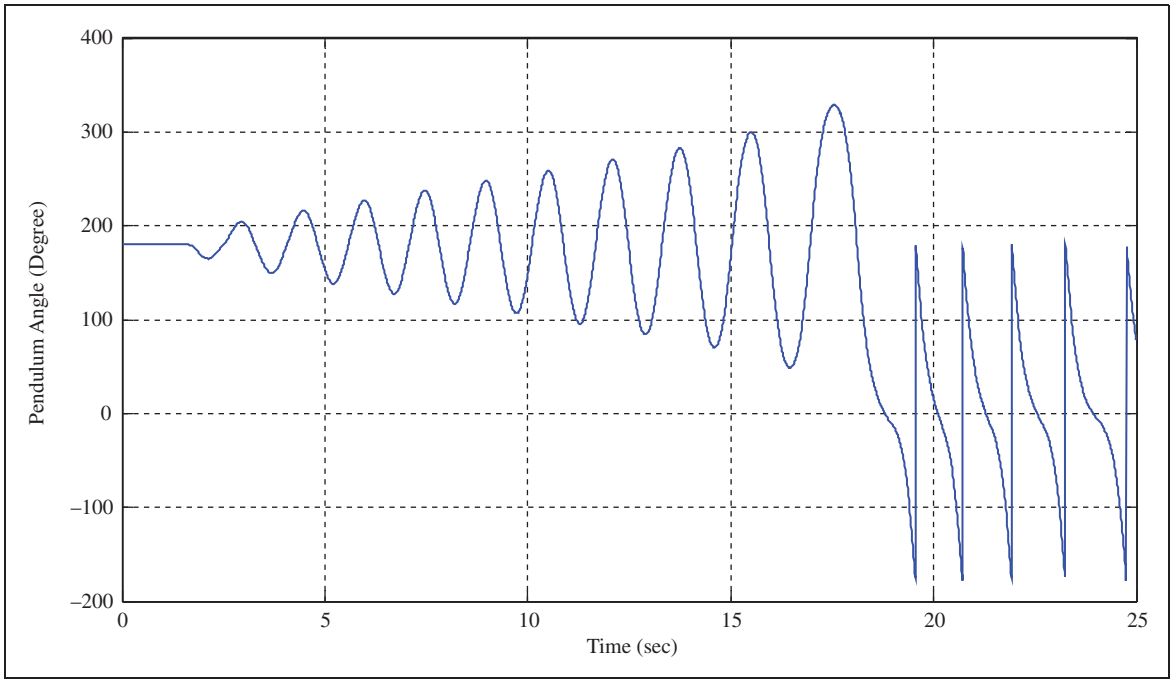

Figure 8. Experimental results without stabilizer for system performance.

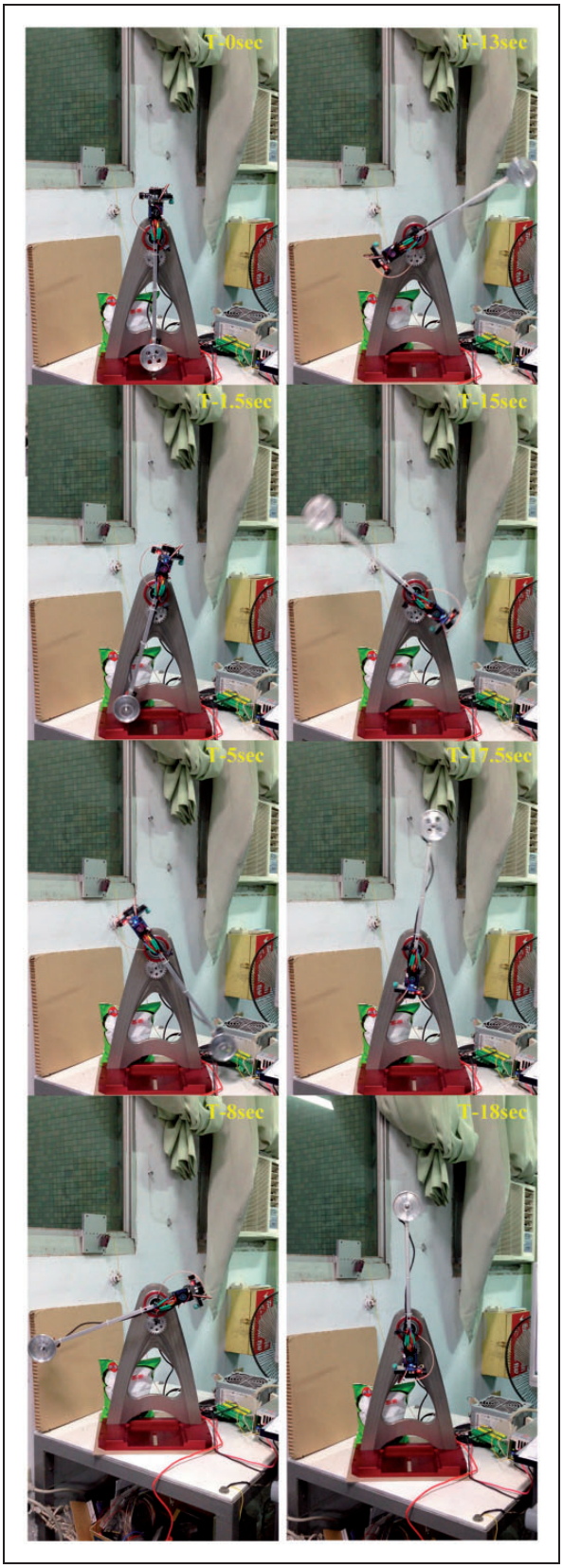

Figure 9. Swing-up, standing-up, and balancing behavior tests in the experiment.

moments of inertia are made possible by using the following simplified formulas:

$$l = 0.2\,\text{m}, \quad m_p = 0.070\,\text{kg}, \quad m_f = 0.231\,\text{kg}$$
$$J_p = 0.0009\,\text{kg}\cdot\text{m}^2, \quad J_f = 0.0001\,\text{kg}\cdot\text{m}^2.$$

5.2. Experimental results

This section summarizes the experimental results to demonstrate the feasibility of applying the proposed controller. The hybrid control strategy for stabilization of the inertia flywheel pendulum is presented and examined. Several experiments validate the effectiveness of the proposed scheme. The calculation for control results is obtained by the procedures introduced in Section 4. The GA scheme can generalize several pairs and optimize the control gains for the balancing purposes based on the approximated transfer function.

Figure 8 shows the swing-up behaviors only with an energy-based control strategy and without a stabilizer. Obviously, performance of the swing-up is deteriorated while the pendulum swings-up to a neighborhood of the top position. Hence, a stabilization controller for this system is highly desirable.

Figure 9 shows the swing-up, standing-up, and balancing behaviors, as evaluated by the proposed control scheme. Figure 10 summarizes the experimental results with the proposed hybrid control for a pendulum angle, angular velocity of the pendulum, and motor control signal, respectively. The switching function in Figure 10 indicates which controller is active. The GA PID controller is active during both the initial push-off and the final balance phase. The swing-up actions continue for 18 seconds before the switching controller activates the stabilization controller. Figure 9 indicates that the pendulum is entirely balanced in its top vertical position within 19 seconds. Moreover, according to the plots in Figure 10, the time history of the pendulum angle tends to move rapidly to the neighborhood of the reference value. Similarly, even if the system has unexpected disturbance at 12 seconds, the experimental results also demonstrates that GA PID can maintain the pendulum in the inverted position (Figure 11).

Moreover, the experimental results demonstrate the damping oscillation ability of such a system that incorporates the proposed hybrid control strategy. While the pendulum freefalls down from the top equilibrium point, the time history of the pendulum angle tends to move rapidly towards the downward position by introducing the GA PID stabilization controller. Figure 12 summarizes the experimental results of the system behaviors with and without the stabilizer for

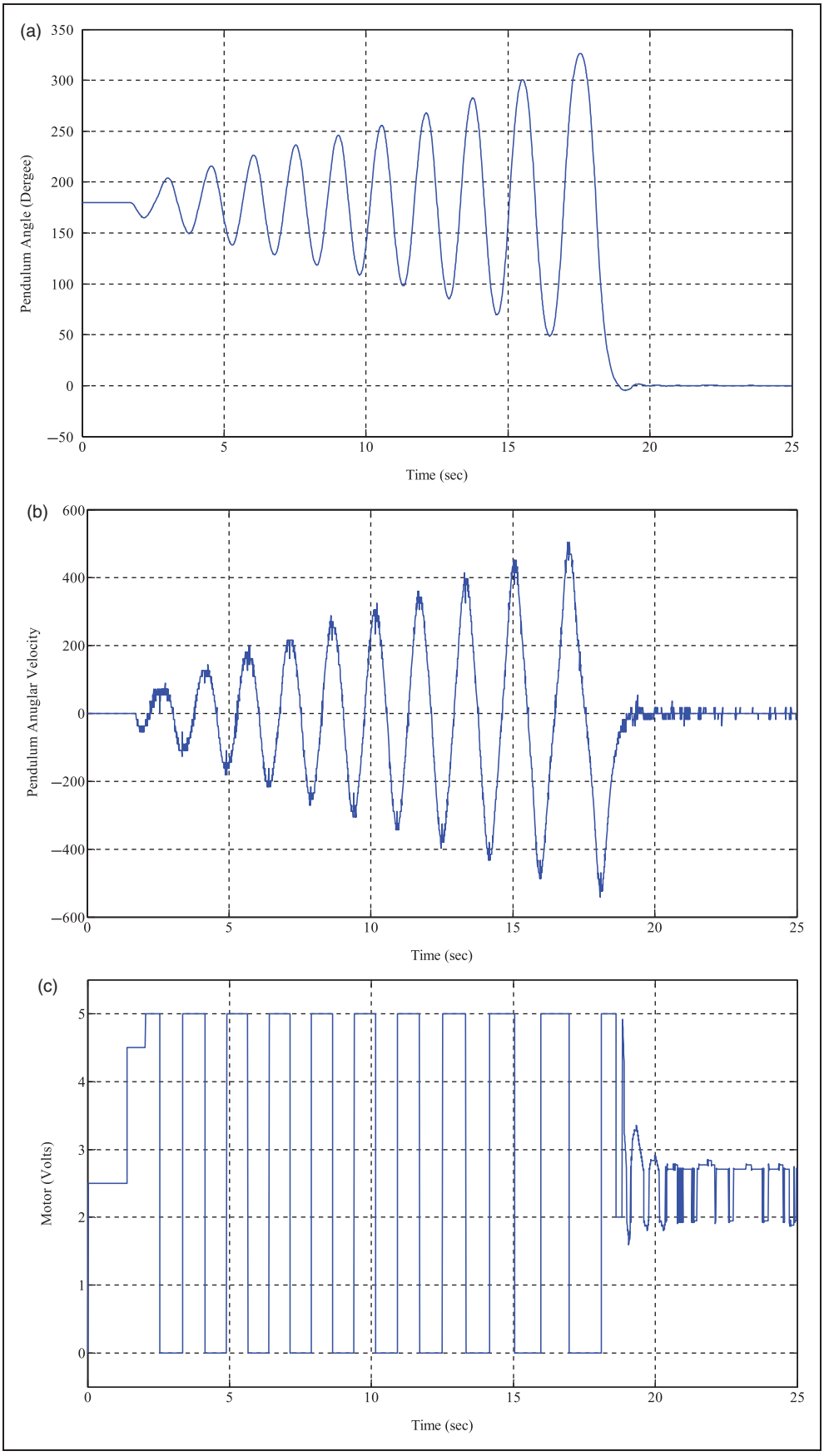

Figure 10. Experimental results with the proposed hybrid control. (a) Pendulum angle; (b) Angular velocity of the pendulum; (c) Motor control signal.

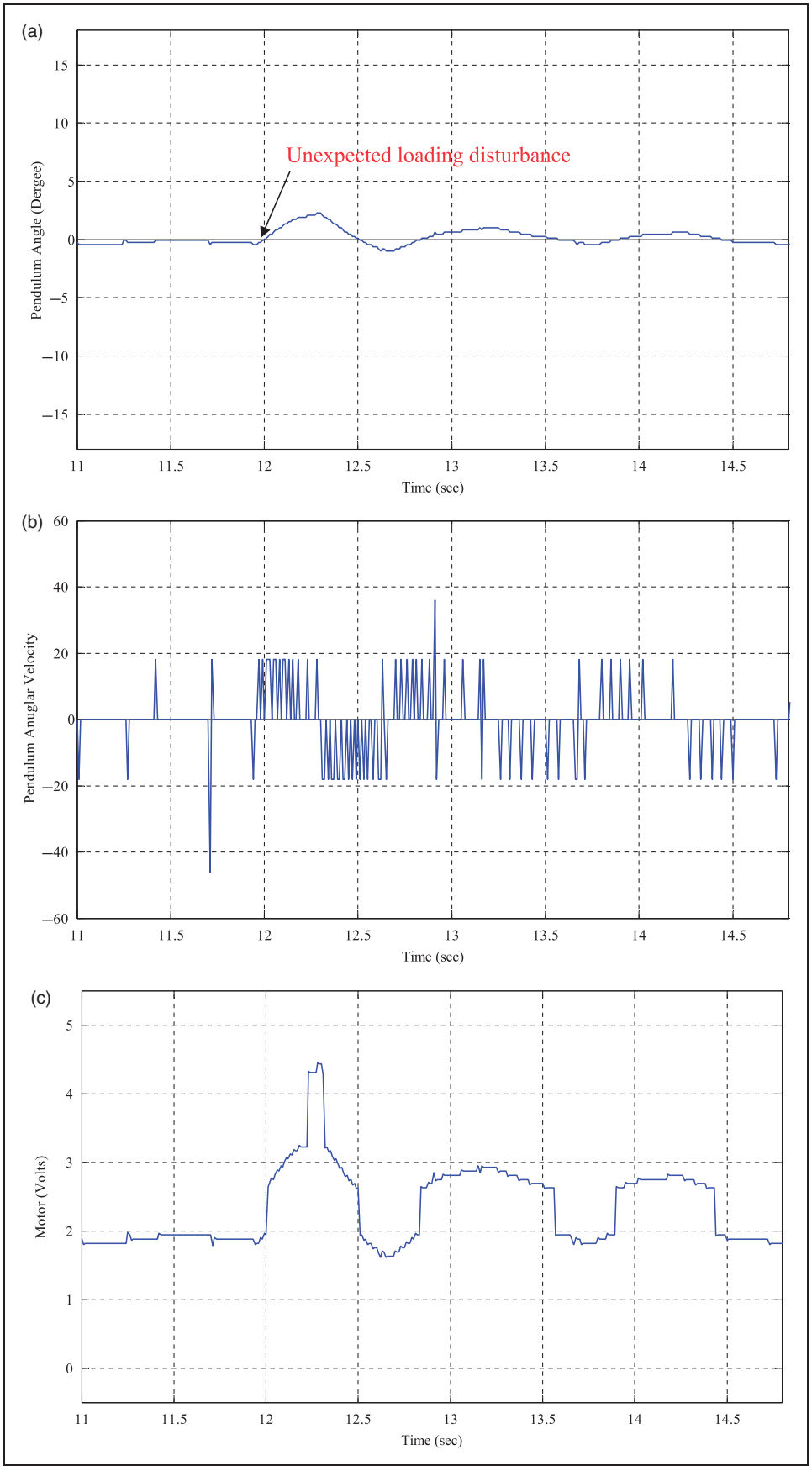

Figure 11. Experimental results with the proposed hybrid control under unexpected loading disturbance. (a) Pendulum angle; (b) Angular velocity of the pendulum; (c) Motor control signal.

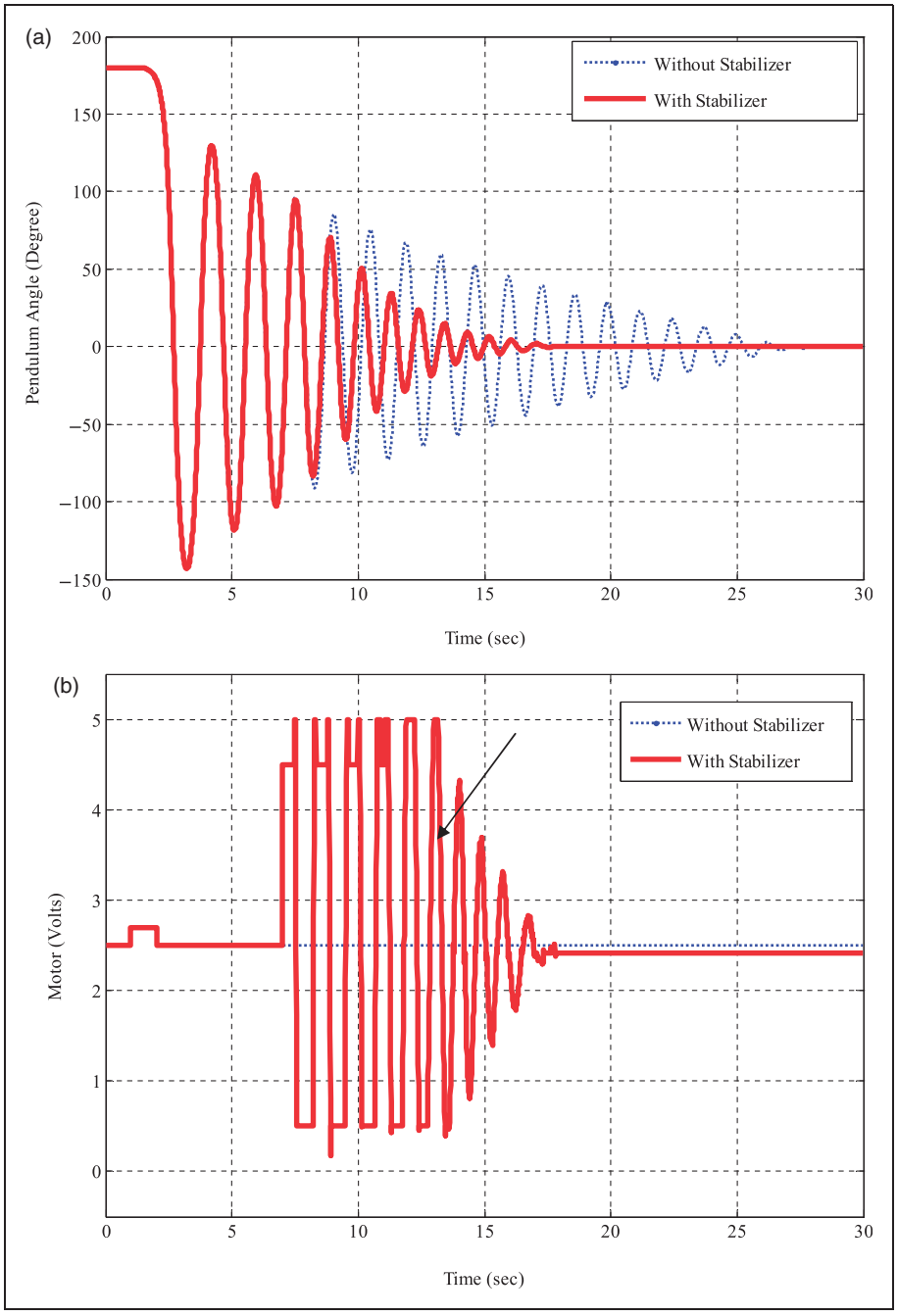

Figure 12. Experimental results with and without stabilizer for physical swing of the pendulum from the top equilibrium point. (a) Pendulum angle; (b) Motor control signal.

physical swings of the pendulum from the top equilibrium point. The controlled angle response confirms that the stabilization PID controller tuned by the GA can effectively suppress the oscillation of the pendulum. This control scheme eliminates oscillation of the system and quickly dampens the swing phenomenon.

Based on the above experimental results, it is concluded that the proposed hybrid control methodology successfully achieves stabilization control, even with unanticipated loading conditions. The fact that changes to system parameters only slightly affect the performance of the hybrid controller demonstrates the effectiveness of the proposed controller in minimizing tracking errors in the time domain, even when the system is caused by loading conditions. Experimental results indicate that the proposed control method suppresses the tracking errors effectively. In contrast to conventional PID control methods, the proposed GA

PID control methodology is robust for parameter changes and other system disturbances.

6. Conclusions

This paper presents a novel mechatronic kit with a control methodology for an inertia flywheel pendulum. The restoring torque depends on the movement of the flywheel and the DC motor has to be run in a Min-Max voltage limit. Moreover, this study also discussed hybrid control of an inertia flywheel pendulum system to achieve swing-up, standing-up, and balancing. The hybrid control strategy for stabilization of the inertia flywheel pendulum is presented and examined. The control aim is achieved by the solution of the following two particular control problems: swinging the pendulum up to a certain neighborhood of the inverted position and balancing it in this position. For the design of a swing-up controller, energy control was adopted. The second aim was achieved by means of a GA PID controller. Hence, the proposed hybrid control methodology has successfully performed stabilization control, even when unexpected loading conditions occur. It is robust for parameter changes and other disturbances in the system. Experimental results in the actual process have shown that the proposed control method suppressed the tracking error effectively. Consequently, the proposed inertia flywheel inverted pendulum is a novel and challenging plant for the design and testing of several control synthesis techniques. It is ideally suited in advanced control courses for educating university students.

Acknowledgements

The authors would like to thank their funding body, and Ted Knoy is appreciated for his editorial assistance.

Funding

This work was partially supported by the National Science Council of the Republic of China, Taiwan (contract number NSC 101-3113-S-231-002).

Nomenclature

E	total energy of the system
E_r	reference energy of the system in swing-up control mode
$\mathbf{G}_{CL}(s)$	second-order transfer function
$H(\theta_p, \dot{\theta}_p)$	objective function for swing-up control mode
J	total inertia moment of the system
J_f	moment of inertia of the flywheel around its center of mass
J_p	moment of inertia of the pendulum around its center of mass
K	total kinetic energy of the system
l	distance from pivot to the center of mass of the pendulum and the flywheel
m_f	mass of the flywheel
m_p	mass of the pendulum
P	total potential energy of the system
u	motor torque input applied on the flywheel
u_1	energy control (swing-up) input
u_2	stabilization control action
γ	an arbitrary positive constant
θ_p	angle of the pendulum
θ_f	angle of the flywheel
θ_s	pendulum angle when switching has occurred between two algorithms
θ^*	desired pendulum angle
ω_p	frequency of oscillation for the pendulum in small amplitudes

References

Aguilar LT, Boiko I, Fridman L and Freidovich L (2009) Inducing oscillations in an inertia wheel pendulum via two-relays controllers: theory and experiments. In *Proceedings of the American Control Conference*, St. Louis, Missouri, USA 10–12 June, pp. 65–70.

Aoustin Y, Formal'sky AM and Martynenko Y (2005) A flywheel to stabilize a two-link pendulum. In: *Proceedings of the 16th IFAC World Congress*, Prague, Czech Republic, 4–8 July.

Aoustin Y, Formal'sky A and Martynenko Y (2006) Stabilization of unstable equilibrium postures of a two-link pendulum using a flywheel. *International Journal of Computer and System Science* 45(2): 204–211.

Block DJ, Åström KJ and Spong MW (2007) *The Reaction Wheel Pendulum*. USA: Morgan & Claypool.

Chetouane F and Darenfed S (2008) Neural network NARMA of a gyroscopic inverted pendulum. *Engineering Letters* 16(3): 274–279.

Chetouane F, Darenfed S and Singh PK (2010) Fuzzy control of a gyroscopic inverted pendulum. *Engineering Letters* 18(1): 10–17.

Fantoni IR, Lozano R and Spong MW (2001) Stabilization of the reaction wheel pendulum using and energy approach. In *Proceedings of the European Control Conference*, Porto, Portugal, 4–7 September, pp. 2552–2557.

Formal'sky AM (2006) An inverted pendulum on a fixed and a moving base. *Journal of Applied Mathematics and Mechanics* 70(1): 62–71.

Grishin AA, Lenskii AV, Okhotsimsky DE, Panin DA and Formal'sky AM (2002) A control synthesis for an unstable object – an inverted pendulum. *Computer and System Sciences International* 41(5): 685–694.

Lam PY (2011) Gyroscopic stabilization of a kid-size bicycle. In: *2011 IEEE 5th International Conference on Cybernetics and Intelligent System* (*CIS*), Qingdao, China, 17–19 September, pp. 247–52.

Li Z and Yang C (2012) Neural-adaptive output feedback control of a class of transportation vehicles based on wheeled inverted pendulum models. *IEEE Transactions on Control System Technology* 20(6): 1583–1591.

Lin J and Zheng YB (2012) Vibration suppression control of smart piezoelectric rotating truss structure by parallel neuro-fuzzy control with genetic algorithm tuning. *Journal of Sound and Vibration* 331(26): 3677–3694.

Pyrkin AA, Bobtsov AA and Kolyubin SA (2009) Stabilization of reaction wheel pendulum on movable support with on-line identification of unknown parameters. In *Proceedings of 4th International Conference on Physics and Control*, Catania, Italy, 1–4 September.

Ruan XG and Wang YF (2010) The modeling and control of flywheel inverted pendulum system. In *Proceedings of 3rd International Conference on Computer Science and Information Technology*, Chengdu, China, 9–11 July, pp. 423–427.

Spong MW, Corke P and Lozano R (2001) Nonlinear control of the reaction wheel pendulum. *Automatica* 37(11): 1845–1851.

Srinivas KN and Behera L (2008) Swing-up control strategies for a reaction wheel pendulum. *International Journal of System Science* 39(12): 1165–1177.